General spin-order theory via gauge Landau-Lifshitz equation

You-Quan Li, Ye-Hua Liu, and Yi Zhou

Zhejiang Institute of Modern Physics and Department of Physics, Zhejiang University, Hangzhou 310027, People's Republic of China

(Received 23 October 2011; published 16 November 2011)

The continuum limit of the tilted SU(2) spin model is shown to lead to a gauge Landau-Lifshitz equation which provides a unified description for various spin orders. For a definite gauge with zero field strength, we find a double periodic solution, where the conical spiral, in-plane spiral, helical, and ferromagnetic spin orders become special cases. For another gauge with nonzero field strength, we obtain the skyrmion-crystal solution. By simulating the influence of magnetic field and temperature for our model, we find a spontaneous formation of a skyrmion-fragment lattice similar to the spin texture found in experiment very recently; we also obtain a wider range of skyrmion-crystal phase in the parameter space in comparison to the conventional Dzyaloshinsky-Moriya model.

DOI: 10.1103/PhysRevB.84.205123 PACS number(s): 75.10.Jm, 75.10.Pq, 75.30.Gw, 75.85.+t

I. INTRODUCTION

There has been spectacular progress in the study of magnetoelectric effects, from which a realistic step toward an electrical control of magnetism is expected to be made.[1–5] Within the intertwining of theory and experiment, a mechanism based on spin current showed that the enhanced ferroelectric domains can be realized through cycloidal and conical spin textures in certain materials.[2,6] For example, a spiral spin state was shown to cause electronic polarization.[6–9] Those nontrivial spin textures undoubtedly play an important role in novel multiferroic materials, so the search for novel spin textures in various materials becomes a central issue in this field. Moreover, the statical and dynamical properties of nontrivial spin textures are interesting in their own right. Recently, the skyrmion[10] lattice phase was predicted[11] in theory and observed experimentally in bulk MnSi (Refs. 12 and 13) and thin film $Fe_xCo_{1-x}Si$ (Ref. 14) and FeGe (Ref. 15). The skyrmion lattice phase in these systems is stabilized by an applied magnetic field. Very recently, a spontaneous skyrmion lattice without a magnetic field is also observed in thin films experimentally.[16] Because of the topological nontrivial property of skyrmions, materials in the skyrmion phase also show novel transport properties like the "topological Hall effect"[17,18] and the "skyrmion Hall effect."[19] Spin dynamical properties like magnons in helical magnets are also probed by neutron scattering experiments,[20] the underlying symmetry of the helical spin order causes magnons to form a band structure.

Theoretically, there are mainly two kinds of mechanisms that cause spiral spin states, one is a ferro/antiferro-magnetic exchange competition that is believed to be the origin of spiral state in manganites[21] and the other is the antisymmetric Dzyaloshinsky-Moriya (DM) interaction[22,23] which arises from spin-orbit (SO) interaction and manifests in crystals without inversion symmetry like MnSi. Historically, Moriya[23] was the first to give a microscopic treatment of the DM interaction based on Anderson's superexchange mechanism with SO interaction. Thirty-two years later, Shekhtman *et al.*[24] found that Moriya's theory has a bond-isotropic form if only one takes all the terms up to second order in SO interaction, which has usually been neglected until the present. It is important to set up a unified description for various spin orders.

In this paper, we indicate that the spin system without inversion symmetry can be described by a tilted Heisenberg model in which the tilting is related to the effects associated with bonds. We not only provide a unified description for the known results with new insight into the gauge and geometric point of view but we also obtain a new state, a skyrmion-fragment phase which has been observed experimentally very recently. We illustrate our proposal of the tilted Heisenberg model in the next section and derive the corresponding continuum limit in Sec. III. In Sec. IV, we formulate a gauge Landau-Lifshitz equation from this model and find solutions of various spin textures and derive the dispersion relation of the relevant spin waves. In Sec. V, we investigate the influence of the external magnetic field and temperature and plot the corresponding phase diagram by making use of Monte Carlo simulations. Our conclusion and discussion are given in Sec. VI.

II. TILTED HEISENBERG MODEL

Let L denote the set of points containing all the lattice sites in our system. For bipartite lattice $L = L_A \bigcup L_B$, we can choose the neighborhood $\mathcal{U}^j$ to be the point j and all its nearest-neighbor points, then $\{\mathcal{U}^j | j \in L_A\}$ constitutes a cover of L, i.e., $L = \bigcup_j \mathcal{U}^j$. For example, in a two-dimensional square lattice, $\mathcal{U}^j = \{(j_x - 1, j_y),(j_x, j_y - 1),(j_x, j_y),(j_x, j_y + 1),(j_x + 1, j_y)\}$. In order to reach a unified description of various spin-ordered phases including the situations beyond the traditional ferromagnetic one, we introduce the tilting field U that accounts for any effects arising from spin-orbit coupling or complicated crystalline fields or cumbersome charge order in whatever intricate materials. It is locally defined in the neighborhood $\mathcal{U}^j$, i.e., U_i^j for $i \in \mathcal{U}^j$, so that much richer physics implications can be expressed. We can choose the local frame in such a way that the U field in the center of $\mathcal{U}^j$ is the identity element of the group, i.e., $U_j^j = 1$. Thus we have a much more generalized Hamiltonian,[25]

$$H = -J \sum_{j,j'} \boldsymbol{S}_j \cdot U_{j'}^j \boldsymbol{S}_{j'} \left(U_{j'}^j\right)^{-1}, \tag{1}$$

where $j \in L_A$ and j' refer to the nearest neighbors of j and $\boldsymbol{S}_i$ denotes spin operators at site i. These spin operators,

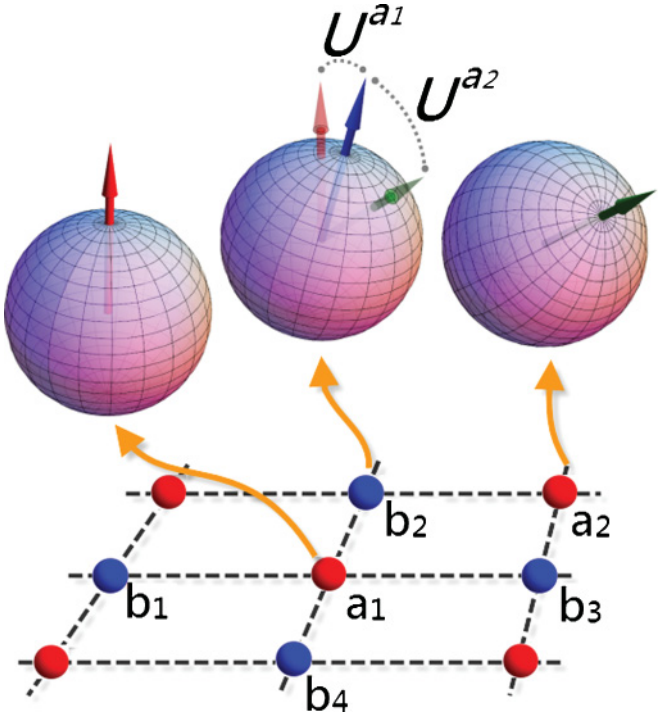

FIG. 1. (Color online) Schematic illustration of the bundle $(L,\mathcal{F},\mathcal{G})$ for the two-dimensional system. The four lattice sites b_1, b_2, b_3, and b_4 in sublattice L_B (blue) and $a_1 \in L_A$ (red) constitute the neighborhood $\mathcal{U}^{a_1}$. In this neighborhood, the tilting fields depict the relative orientation of the polar axes of the Bloch spheres attached on the five sites. The amplified balls above the lattice show, for example, the relative orientation between the ones at a_1 and b_2 that is depicted by the tilting $U^{a_1}_{b_2}$, while the relative orientation between the ones at a_2 and b_2 is depicted by the tilting field $U^{a_2}_{b_2}$ that is defined on another neighborhood $\mathcal{U}^{a_2}$ whose center is a_2. The subscript of the tilting field is omitted for figure neatness.

proportional to the infinitesimal generators of SU(2), obey $[S^a_j, S^b_l] = i\hbar\delta_{jl}\epsilon^{abc}S^c_j$, with $a,b,c = 1,2,3$, which governs the time developments of any observable via the Heisenberg equation of motion for a definite model (1).

Mathematically, our system is defined on a bundle whose base space and typical fiber are, respectively, L and $\mathcal{F}$ which is a Bloch sphere. Each point of L is attached with a fiber $\mathcal{F}$, and the structure group $\mathcal{G}$ that connects nearby fibers is the rotation group. More details of the mathematical concepts can be found, for example, in Ref. 26. We illustrate the physics picture in a two-dimensional lattice in Fig. 1. The tilting $U \in \mathcal{G}$ we introduced is locally defined in each neighborhood, which plays a crucial role in bringing in various exotic spin orders. Thus we call the model the tilted Heisenberg model.

III. THE CONTINUUM LIMIT

As there exists a homomorphism between SU(2) and SO(3) Lie groups, $U^j_{j'}\boldsymbol{S}_{j'}(U^j_{j'})^{-1} = \boldsymbol{S}_{j'}O^j_{j'}$ in which $\boldsymbol{S}_{j'}$ denotes $(S^1_{j'}, S^2_{j'}, S^3_{j'})$ and $O^j_{j'}$ denotes the representation of SO(3), each nearest-neighbor coupling term in Eq. (1) can be rearranged, i.e., $\boldsymbol{S}_j \cdot U^j_{j'}\boldsymbol{S}_{j'}(U^j_{j'})^{-1} = \boldsymbol{S}_j\,(\boldsymbol{S}_{j'}O^j_{j'})^T = \boldsymbol{S}_j(O^j_{j'})^{-1}\boldsymbol{S}^T_{j'}$. Here $(O^j_{j'})^T = (O^j_{j'})^{-1}$ for the orthogonal group has been used. We consider the coordinate of site j' is simply that of j plus a bond vector $a\boldsymbol{e}_\nu$ in which a denotes the lattice constant and $\boldsymbol{e}_\nu$ refers to the unit vectors connecting the neighborhoods of a given lattice structure. When the lattice constant a is taken as an infinitesimal parameter, $(O^j_{j'})^{-1}$ is then in the vicinity of identity, namely,

$$\left(O^j_{j'}\right)^{-1} = 1 - aA^c_\nu(j)\,\hat{\ell}_c, \tag{2}$$

where O^j_j being identity has been used. Here $\hat{\ell}_c$ denote the representation matrices of the infinitesimal generators of the SO(3) Lie group, they are 3×3 matrices $(\hat{\ell}_c)_{ab} = \epsilon_{abc}$ and fulfill the commutation relations[27] $[\hat{\ell}_a, \hat{\ell}_b] = -\epsilon_{abc}\hat{\ell}_c$. Clearly, the feature of the local tilting can be characterized by the SO(3) non-Abelian gauge potential $\mathbb{A}_\nu(j) = A^c_\nu(j)\hat{\ell}_c$, which is a matrix valued vector field. In order to avoid any ambiguity, here we clarify that the j represents a point in the lattice space corresponding to the coordinate of real space in the continuum model, and the c labels the component of a vector in Lie algebra space while the ν labels the one in real space. Also for symbol neatness, in Eq. (2) and thereafter, we write the lattice-site label j of A in parentheses rather than conventional subscripts. By making use of Eq. (2), we can write Eq. (1) as

$$H = \frac{J}{2}\sum_{jj'}\left[\left(\boldsymbol{S}_{j'} - \boldsymbol{S}_j + a\boldsymbol{S}_jA^c_\nu(j)\,\hat{\ell}_c\right)^2 - 2C_j\right]. \tag{3}$$

Actually, the Casimir invariants $C_j = \boldsymbol{S}_j\cdot\boldsymbol{S}_j = s_j(s_j+1)\hbar^2$ in a general system may differ at different lattice site, which means the module of spin does not necessarily take the same value everywhere. However, in this paper, we focus on uniform spin module S in every site.

Now we are in a position to make the continuum limit, $\sum \to (1/a)^d\int \mathrm{d}^dx$, which can be realized by allowing the volume per lattice site a^d to tend to zero and considering the lattice label j as a continuous variable $\boldsymbol{r}$ and hence $\boldsymbol{S}_j$ as $\boldsymbol{M}(\boldsymbol{r})$. Equation (3) gives rise to the effect Hamiltonian,

$$H = \frac{J}{2a^{d-2}}\int \mathrm{d}^dx[(\partial_\nu + \boldsymbol{A}_\nu(\boldsymbol{r})\times)\boldsymbol{M}(\boldsymbol{r})]^2, \tag{4}$$

where the additional constant term is omitted. If we expand the quadratic term, we obtain the energy density,

$$\mathcal{H} = \frac{J}{2a^{d-2}}[(\partial_\nu\boldsymbol{M})^2 + 2\boldsymbol{A}_\nu\cdot(\boldsymbol{M}\times\partial_\nu\boldsymbol{M}) + (\boldsymbol{A}_\nu\times\boldsymbol{M})^2], \tag{5}$$

where the three terms can be interpreted as a ferromagnetic exchange term, the conventional DM term, and a single ion anisotropic term, respectively. A conventional model in the literature of the DM interaction is readily a special case of our formulation. If substituting $A_x = (-\gamma/J,0,0)$, $A_y = (0,-\gamma/J,0)$, and $A_z = (0,0,-\gamma/J)$ into the Eq. (4) in three dimensions, we have

$$H = \int d^3x\left[\frac{J}{2a}(\nabla\boldsymbol{M})^2 + \frac{\gamma}{a}\boldsymbol{M}\cdot(\nabla\times\boldsymbol{M})\right]$$

up to a constant in energy. This Hamiltonian was used to explain the appearance of a skyrmion lattice.[13,14]

IV. GAUGE LANDAU-LIFSHITZ EQUATION

The Lagrangian density corresponding to the Hamiltonian (4) is given by

$$\mathcal{L} = a^{-d}|\boldsymbol{M}|(\cos\theta - 1)\dot{\phi} - a^{2-d}J/2\,(D\boldsymbol{M})^2,$$

in which (θ,ϕ) refer to the azimuthal angles of $\boldsymbol{M}$. The equation of motion for the spin field $\boldsymbol{M}(\boldsymbol{r},t)$ is derived by

$$\mathbf{M} \times \frac{\delta}{\delta \mathbf{M}} \int d^d x dt\, \mathcal{L} = 0$$

as the following gauge Landau-Lifshitz equation,

$$\frac{\partial}{\partial t}\boldsymbol{M} = a^2 J \boldsymbol{M} \times D^2 \boldsymbol{M}, \tag{6}$$

where $D^2 = D_\nu D_\nu$ and the covariant derivative is given by $D_\nu \boldsymbol{M} = (\partial_\nu + \boldsymbol{A}_\nu \times)\boldsymbol{M}$. Equation (6) is covariant under a gauge transformation:

$$\mathbb{A}_\nu \to G\mathbb{A}_\nu G^{-1} + \partial_\nu G G^{-1},$$
$$(\boldsymbol{M})_a \to \sum_b G_{ab}(\boldsymbol{M})_b,$$

where $G \in \mathrm{SO}(3)$.

A. Double periodic solutions in two dimensions

We first consider a typical gauge field in the x-y plane: $\boldsymbol{A}_x = (0,0,-q_1)$ and $\boldsymbol{A}_y = (q_2 \sin q_1 x, -q_2 \cos q_1 x, 0)$. We find a double periodic solution, $\boldsymbol{M}_{\mathrm{dp}}$, as a steady solution of the gauge Landau-Lifshitz equation (6):

$$\begin{cases} m_1(x,y) = \sin(q_2 y + \beta)\cos(q_1 x), \\ m_2(x,y) = \sin(q_2 y + \beta)\sin(q_1 x), \\ m_3(x,y) = \cos(q_2 y + \beta). \end{cases} \tag{7}$$

Here $\boldsymbol{m} = (m_1,m_2,m_3)$ refers to $\boldsymbol{M}_{\mathrm{dp}}/S$. A schematic illustration of the solution (7) is depicted in Fig. 2. This spin order is the exact ground-state solution of the system because $D_x \boldsymbol{M}_{\mathrm{dp}} = D_y \boldsymbol{M}_{\mathrm{dp}} = 0$ so that the positive definite energy functional (4) reaches zero then. Clearly, the conical spiral spin order[28] is the special case of $q_2 = 0$, whose special case of $\beta = \pi/2$ reduces to the in-plane spiral spin order.[29] The other cases $q_1 = 0$ or $q_1 = q_2 = 0$ correspond to the helical spin order[30] or the ferromagnetic spin order, respectively.

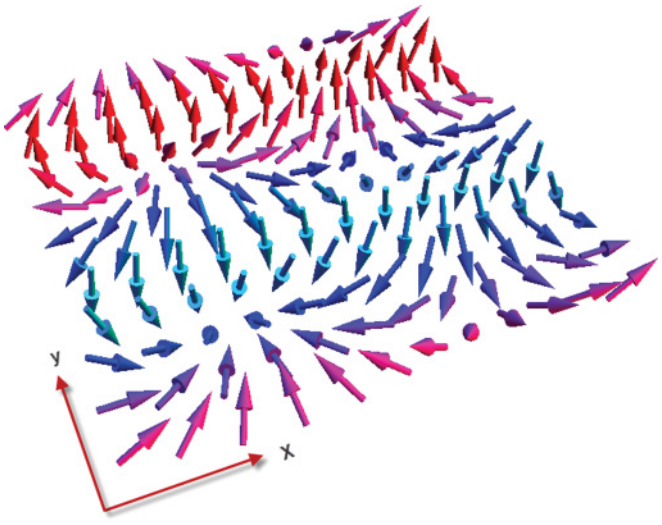

FIG. 2. (Color online) Schematic illustration of the spin order for the double periodic solution of the gauge Landau-Lifshitz equation.

To study the excitations above the aforementioned ground state (7), we take $\boldsymbol{M}_{\mathrm{dp}} + \delta\boldsymbol{M}$ and obtain the linearized equation $(\partial_t - a^2 J \boldsymbol{M}_{\mathrm{dp}} \times D^2)\delta\boldsymbol{M} = 0$. Since the constraint $|\boldsymbol{M}| = S$ requires $\boldsymbol{M}_{\mathrm{dp}} \cdot \delta\boldsymbol{M} = 0$, we can assume $\delta\boldsymbol{M} = u(x,y,t)\boldsymbol{e}_\theta + v(x,y,t)\boldsymbol{e}_\phi$ with the local frame $\boldsymbol{e}_\phi = \boldsymbol{e}_z \times \boldsymbol{M}_{\mathrm{dp}}/|\boldsymbol{e}_z \times \boldsymbol{M}_{\mathrm{dp}}|$ and $\boldsymbol{e}_\theta = \boldsymbol{e}_\phi \times \boldsymbol{M}_{\mathrm{dp}}/|\boldsymbol{e}_\phi \times \boldsymbol{M}_{\mathrm{dp}}|$. Then the equations that possible low-lying excitation modes obey are

$$\partial_t u + a^2 J S \nabla^2 v = 0, \quad \partial_t v - a^2 J S \nabla^2 u = 0. \tag{8}$$

Their Fourier transform gives rise to the dispersion relation $\omega^2 = a^4 J^2 S^2 |\boldsymbol{k}|^4$. One can see that the dispersion relation here happens to be the same as that of the spin wave above a ferromagnetic ground state in the classical Heisenberg model.

Because the strength tensor $F^c_{xy} = \partial_x A^c_y - \partial_y A^c_x + \epsilon^{abc} A^a_x A^b_y$ vanishes for the gauge potential relevant to the solution (7), the gauge potential can be represented as a pure gauge $\mathbb{A}_\nu = -G^{-1}\partial_\nu G$, with $G = \exp(q_2 y \hat{\ell}_2)\exp(q_1 x \hat{\ell}_3)$. The generating matrix G implies an important physical significance, which transforms the double periodic spiral order (7) to the traditional ferromagnetic order, i.e., $(\boldsymbol{M}_{\mathrm{fe}})_a = \sum_b G_{ab}(\boldsymbol{M}_{\mathrm{dp}})_b$. Here $\boldsymbol{M}_{\mathrm{fe}}$ is the ground-state solution of Eq. (6) with zero gauge potential. The double periodic spiral order can be considered as a result of parallel displacement of spin with the aforementioned gauge potential as a connection. Since the solutions referring to both orders are in the same equivalent class of gauge Landau-Lifishitz equation, it should be no surprise that the dispersion relations for the excitations above them are the same.

B. Skyrmion crystal solution in two dimensions

The previous solution is related to a gauge potential with vanishing strength tensor. Let us now investigate the case with nonvanishing strength tensor, which gives rise to skyrmion[10] crystal solutions. For $\boldsymbol{A}_x = (-\gamma/J,0,0)$ and $\boldsymbol{A}_y = (0,-\gamma/J,0)$, where γ denotes the strength of spin-orbit interaction, we have $\boldsymbol{F}_{xy} = (0,0,\gamma^2/J^2)$ and energy density

$$\mathcal{H} = (J/2)\partial_\nu \boldsymbol{M} \cdot \partial_\nu \boldsymbol{M} + \gamma \boldsymbol{M} \cdot (\nabla \times \boldsymbol{M}) + (\gamma^2/2J)[\boldsymbol{M}^2 + (M_3)^2]. \tag{9}$$

Here the last term contributes an easy-plane anisotropy that is the continuum version of Moriya's anisotropic exchange;[23] the first two terms are the conventional ferromagnetic exchange and the DM interaction which was used to explore possible states of skyrmion crystal.[14,31] Unlike the solution of double periodic spiral order which can be generated through a parallel displacement (no parallel displacement can be globally defined if the field strength is nonzero), we need to solve the gauge Landau-Lifshitz equation at present.

For steady solution of the gauge Landau-Lifshitz equation (6), it is sufficient to solve the eigenequation $D^2\boldsymbol{M} = \lambda\boldsymbol{M}$. The λ can be a scalar function in general whereas it is assumed to be a constant here for simplicity. It can be proven that the λ is proportional to the energy density. Being interested in a periodic steady solution, we can assume $\boldsymbol{M}(\boldsymbol{r}) = \boldsymbol{M}(\boldsymbol{k})\exp(i\boldsymbol{k}\cdot\boldsymbol{r})$.

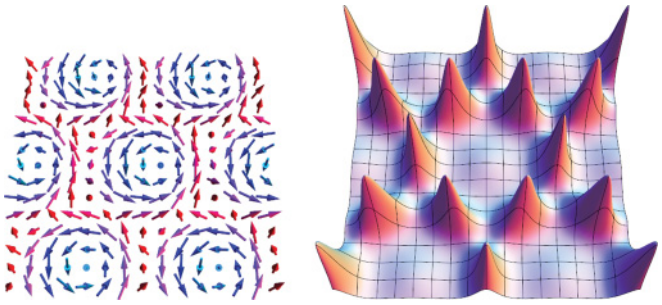

FIG. 3. (Color online) Schematic illustration for spin order of skyrmion-crystal solution (left panel) and the corresponding distribution of energy density in the zero magnetic field (right panel). The energy density is lower at the center of skyrmion because the local spin chirality is large there, which is favored by the DM interaction; it is larger in the boundaries of skyrmions but the spins there favor a perpendicular magnetic field.

Then the eigenequations become a set of algebraic equations for us to determine $\boldsymbol{M}(\boldsymbol{k})$. We obtain three solutions: sinusoidal order with spin paralleling the wave vector and elliptically distorted right-handed and left-handed helical orders with spin perpendicular to the wave vector. As the three eigenvalues depend on $|\boldsymbol{k}|^2$ merely, we can make superpositions of the eigenmodes corresponding to the same eigenvalue. In the present case, $\gamma > 0$ is assumed, so we want to choose the right-handed helical order to construct the ground state. The closest-packed lattice of skyrmions are superpositions of three such eigenmodes with three wave vectors of the same length and mutually in 120° angle, namely, $\boldsymbol{M}_c = \sum_{i=1}^{3} \boldsymbol{M}(\boldsymbol{k}_i)e^{i\boldsymbol{k}_i\cdot\boldsymbol{r}}$ in which $\boldsymbol{k}_1 = (\frac{\sqrt{3}}{2}k, \frac{1}{2}k)$, $\boldsymbol{k}_2 = (-\frac{\sqrt{3}}{2}k, \frac{1}{2}k)$, and $\boldsymbol{k}_3 = (0, -k)$. Since the real and imaginary parts of $\boldsymbol{M}_c$ all satisfy Eq. (6), we can normalize the real part to reach a physical state that is a compromise of reducing energy and satisfying the unit-length constraint, $\boldsymbol{m}_{\rm sk} = {\rm Re}(\boldsymbol{M}_c)/|{\rm Re}(\boldsymbol{M}_c)|$. Here the unfixed parameter k in $\boldsymbol{m}_{\rm sk}$ determines the lattice constant of the skyrmion crystal.

The particular k is determined by minimizing the average energy density which is calculated through numerical integration. Some features of the solution are plotted in Fig. 3 where spins between the center of skyrmions tend to point up although the spins in each skyrmion tend to point down. The average energy density of the optimized configuration of the skyrmion crystal is $0.276S^2\gamma^2/J$ with $k = 0.87\gamma/J$, higher than the helical order's $0.25S^2\gamma^2/J$, but the average z component of spin for the solution $\boldsymbol{m}_{\rm sk}$ is $+0.17$. The skyrmion crystal will have lower energy when a sufficiently large perpendicular magnetic field is applied downward. Whereas, when the magnetic field is further enhanced, a ferromagnetic state with the z component of spin being 1 eventually becomes the ground state. This argument is consistent with a recent reference.[14]

C. The influence of anisotropy

Furthermore, we study what will happen if there exists a magnetic anisotropy in the system. Such an anisotropy can be introduced by adding the term $\sum_j \eta(S_j^z)^2$ in the tilted spin model (1) in which either the easy axis is chosen as the z axis or the easy plane is chosen as as the x-y plane for $\eta < 0$ or $\eta > 0$, respectively. Choosing this kind of anisotropy is due to keeping the original rotational symmetry about the z axis. Then the above gauge Landau-Lifshitz equation (6) turns to the following anisotropic one,

$$\frac{\partial}{\partial t}\boldsymbol{M} = a^2 J\boldsymbol{M}\times D^2\boldsymbol{M} - 2\eta\boldsymbol{M}\times\boldsymbol{M}', \tag{10}$$

with $\boldsymbol{M}' = (0,0,M_z)$. Note that the gauge potential with the skyrmion-crystal solution merely contributes an easy plane anisotropy. When the anisotropy coexists with the aforementioned gauge potential relevant to the skyrmion-crystal solution, the eigenequation for the original gauge Landau-Lifshitz equation in k space is modified. One can choose the right-handed helical mode $(k_y, -k_x, i\rho|\boldsymbol{k}|)$ in which $\rho = \sqrt{\xi^2+1} - \xi$, where $\xi = (\gamma^2 + 2J\eta/a^2)/(4J\gamma|\boldsymbol{k}|)$. In real space, this mode is a helical order of elliptic contour with ρ referring to the ratio of semiminor and semimajor axes. It can be seen that the larger the η is, the smaller the ρ will be, which is in consistent with the requirement for minimizing the energy. When $\xi = 0$ we have $\rho = 1$; this causes a cancellation between the added anisotropy term and the second-order term of γ arising from the gauge potential.

V. FINITE TEMPERATURE EFFECTS

Now we turn to investigate finite temperature effects of our covariant model which contains the DM interaction and magnetic anisotropy simultaneously. For convenience in numerical simulation, we start from the lattice version that is discretized from the Hamiltonian (4) for $A_x = (-K/J, 0)$ and $A_y = (0, -K/J)$ together with a Zeeman term, namely,

$$H = \sum_{\boldsymbol{r},\boldsymbol{e}}[-J\boldsymbol{S}_{\boldsymbol{r}}\cdot\boldsymbol{S}_{\boldsymbol{r}+a\boldsymbol{e}} - K\boldsymbol{e}\cdot(\boldsymbol{S}_{\boldsymbol{r}}\times\boldsymbol{S}_{\boldsymbol{r}+a\boldsymbol{e}})] + \sum_{\boldsymbol{r}}\left[\frac{K^2}{2J}\left(S_{\boldsymbol{r}}^z\right)^2 - BS_{\boldsymbol{r}}^z\right], \tag{11}$$

where $\boldsymbol{S}$ denotes the classical spin of the unit module; $\boldsymbol{e}$ refers to $\hat{x}$ or $\hat{y}$ and $\boldsymbol{r}$ runs through the lattice site of the base space; J, K, and B denote the exchange, the strength of the DM interaction, and the external magnetic field, respectively. In our numerical calculation, the Boltzmann constant k_B and the lattice spacing a are taken as a unit. We do Monte Carlo simulations with periodic boundary conditions in various regimes of model parameters.

For the zero magnetic field $B = 0$, we find, for a specific strength of the DM interaction $K/J = \sqrt{2}\tan(2\pi/6)$, the system goes from disordered phase to helical phase and then to a new phase when temperature is lowering. The new phase (see Fig. 4) presents a square lattice of alternatively placed skyrmion fragments, some of which appear to be embedded among spin helical textures, that is marked by black dotted lines in Fig. 4. In contrast to the usual skyrmion which contains a lot of microspins, the fragment of skyrmion that appears here is atomic scale because each fragment is formed by a 3×3 microspin lattice. Since the new phase appears in the zero magnetic field, it is an emergence of spontaneous formation of a skyrmion-fragment lattice. A similar spin texture has been observed in an experiment very recently.[16]

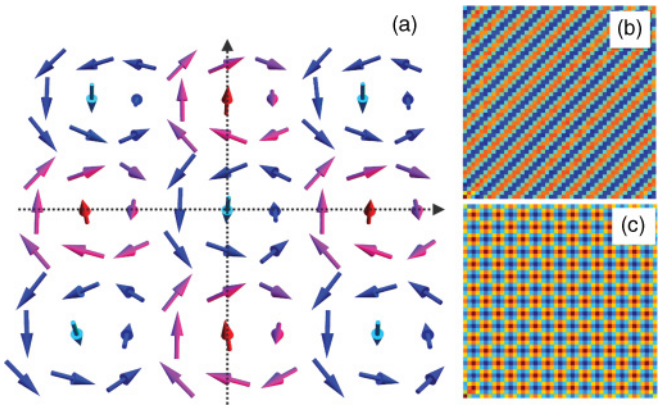

FIG. 4. (Color online) (a) Spin order of the skyrmion-fragment phase. Here is a patch of spin textures from our simulation for $K/J = \sqrt{2}\tan(2\pi/6)$. Along the black dotted-line arrows, the spins form a helical order where each two successive spins have a relative 60° difference in angle. (b) and (c) The spin z-z correlation in the 48 by 48 lattice for various phases in the zero magnetic field. Temperature is lowering, it goes from disordered to helical (b) and then to skyrmion-fragment (c) phases.

For a weaker strength of the DM interaction $K/J = \sqrt{2}\tan(2\pi/9)$, we plot the phase diagrams in the plane of temperature versus the magnetic field based on our Monte Carlo simulations for both our model (11) and the conventional model.[14] The conventional model is our model without the anisotropic term and the typical spin orders involved are plotted in Fig. 5. Our results manifest that the landscape of those two phase diagrams are similar while the area ratio of the skyrmion lattice phase to the helical phase in our model is larger than that in the conventional model (see Fig. 6). Because our model contains an additional anisotropic term, second order to K, it is natural that the larger the K is, the bigger the difference between the result of our model and that of the conventional model will be. When K/J is as large as $\sqrt{2}\tan(2\pi/6)$, our model exhibits a new phase.

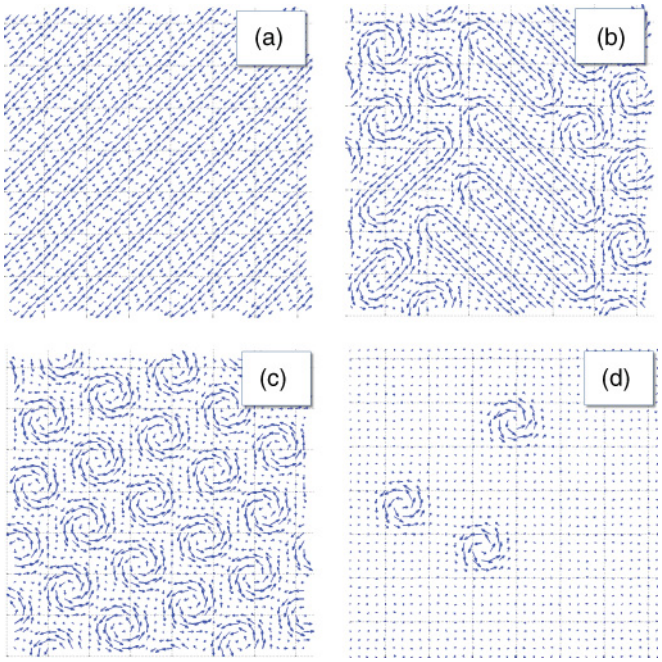

FIG. 5. (Color online) Various spin textures result from Monte Carlo simulation. (a) helical. (b) helical + skyrmion. (c) skyrmion lattice and (d) ferromagnetic + skyrmion.

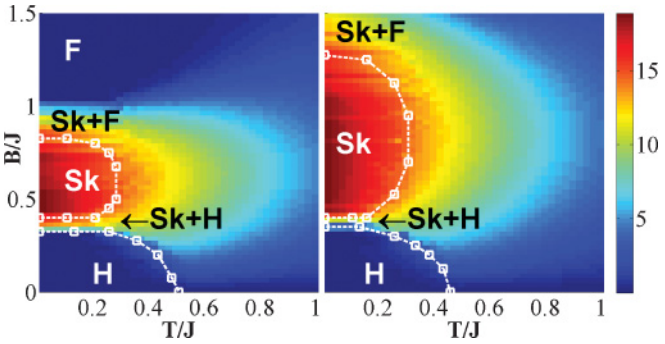

FIG. 6. (Color online) Phase diagram of various spin orders (Sk, skyrmion lattice; H, helical; F, ferromagnetic; +, coexistence) in the plane of the magnetic field versus temperature calculated in the 36 by 36 lattice for the DM model (left panel) and our covariant model (right panel). The color indicates the total number of skyrmions. The helical phase and the ferromagnetic phase have no skyrmions and the skyrmion lattice phase has many skyrmions. In our model the Sk phase occupies more area in the high field region because the intrinsic easy plane anisotropy competes with the magnetic field to prevent the spins from being polarized.

VI. CONCLUSION AND DISCUSSION

In the above, we proposed a tilted Heisenberg model as a general spin-order theory to present various exotic spin orders beyond the traditional ferromagnetic order. In the model, the tilting field plays a crucial role. It is related to the effects associated with bonds from a microscopic point of view and can be more clearly comprehended in terms of mathematical concepts in fiber bundle theory. Furthermore, we formulate the gauge Landau-Lifshitz equation as the continuum limit of the tilted Heisenberg spin model.

We found several static solutions of the gauge Landau-Lifshitz equation and investigated some relevant features. The double periodic solution we found implies the conical spiral, in-plane spiral, helical, and ferromagnetic spin orders as special cases.[28–30] The dispersion relation of the spin wave excitation above the double periodic ground state is shown to be the same as the excitation above ferromagnetic order. This is because the SO(3) gauge potential corresponding to the double periodic solution is a pure gauge (with zero field strength tensor) and such a spin order can be derived by means of parallel displacement of spin. The Hamiltonian that gives double periodic order can be gauge transformed to the ferromagnetic Heisenberg Hamiltonian whose corresponding gauge potential is null in our unified theory. Another class of solution represents the skyrmion-crystal order, which was obtained for a SO(3) gauge with nonvanishing strength tensor.

We also investigated the influence of the external magnetic field and temperature and plotted the corresponding phase

diagram by making use of Monte Carlo simulations. As to the finite temperature behavior, a spontaneous formation of the skyrmion-fragment lattice occurs in zero magnetic field, and the area ratio of the skyrmion phase to the helical phase is larger in our covariant model than in the conventional DM model.[14] The gauge Landau-Lifshitz equation not only provides a unified description for the known results with new insight into the gauge and geometric point of view but also gives a new state, the skyrmion-fragment phase, which has been observed experimentally very recently.[16]

ACKNOWLEDGMENTS

We thank J. H. Han for useful communications. The work is supported by NSFCs (Grants No. 11074216 and No. 11074218) and PCSIRT (Grant No. IRT0754).

[1]M. Fiebig, J. Phys. D **38**, R123 (2005).
[2]Y. Tokura, Science **312**, 1481 (2006).
[3]W. Eerenstein, N. D. Mathur, and J. F. Scott, Nature (London) **442**, 759 (2006).
[4]S.-W. Cheong and M. Mostovoy, Nat. Mater. **6**, 13 (2007).
[5]T. Choi, Y. Horibe, H. T. Yi, Y. J. Choi, W. Wu, and S.-W. Cheong, Nat. Mater. **9**, 253 (2010).
[6]H. Katsura, N. Nagaosa, and A. V. Balatsky, Phys. Rev. Lett. **95**, 057205 (2005).
[7]M. Mostovoy, Phys. Rev. Lett. **96**, 067601 (2006).
[8]C. Jia, S. Onoda, N. Nagaosa, and J. H. Han, Phys. Rev. B **76**, 144424 (2007).
[9]I. A. Sergienko and E. Dagotto, Phys. Rev. B **73**, 094434 (2006).
[10]T. H. R. Skyrme, Nucl. Phys. **31**, 556 (1962).
[11]U. K. Rößler, A. N. Bogdanov, and C. Pfleiderer, Nature (London) **442**, 797 (2006).
[12]C. Pappas, E. Lelièvre-Berna, P. Falus, P. M. Bentley, E. Moskvin, S. Grigoriev, P. Fouquet, and B. Farago, Phys. Rev. Lett. **102**, 197202 (2009).
[13]S. Mühlbauer, B. Binz, F. Jonietz, C. Pfleiderer, A. Rosch, A. Neubauer, R. Georgii, and P. Böni, Science **323**, 915 (2009).
[14]X. Z. Yu, Y. Onose, N. Kanazawa, J. H. Park, J. H. Han, Y. Matsui, N. Nagaosa, and Y. Tokura, Nature (London) **465**, 901 (2010).
[15]X. Z. Yu, N. Kanazawa, Y. Onose, K. Kimoto, W. Z. Zhang, S. Ishiwata, Y. Matsui, and Y. Tokura, Nat. Mater. **10**, 106 (2011).
[16]S. Heinze, K. von Bergmann, M. Menzel, J. Brede, A. Kubetzka, R. Wiesendanger, G. Bihlmayer, and S. Blügel, Nat. Phys. **7**, 713 (2011).
[17]Minhyea Lee, W. Kang, Y. Onose, Y. Tokura, and N. P. Ong, Phys. Rev. Lett. **102**, 186601 (2009).
[18]A. Neubauer, C. Pfleiderer, B. Binz, A. Rosch, R. Ritz, P. G. Niklowitz, and P. Böni, Phys. Rev. Lett. **102**, 186602 (2009).
[19]J. Zang, M. Mostovoy, J. H. Han, and N. Nagaosa, Phys. Rev. Lett. **107**, 136804 (2011).
[20]M. Janoschek, F. Bernlochner, S. Dunsiger, C. Pfleiderer, P. Böni, B. Roessli, P. Link, and A. Rosch, Phys. Rev. B **81**, 214436 (2010).
[21]T. Kimura, S. Ishihara, H. Shintani, T. Arima, K. T. Takahashi, K. Ishizaka, and Y. Tokura, Phys. Rev. B **68**, 060403(R) (2003).
[22]I. Dzyaloshinsky, J. Phys. Chem. Solids **4**, 241 (1958).
[23]T. Moriya, Phys. Rev. **120**, 91 (1960); Phys. Rev. Lett. **4**, 228 (1960).
[24]L. Shekhtman, O. Entin-Wohlman, and A. Aharony, Phys. Rev. Lett. **69**, 836 (1992).
[25]Otherwise, U at site j should also be written out in the Hamiltonian that looks more complicated but is equivalent to Eq. (1). This merely means the same rotation simultaneously for the spin operator at each site in a neighborhood.
[26]B. F. Schutz, *Geometrical Methods of Mathematical Physics* (Cambridge University Press, Cambridge, UK, 1980).
[27]R. Gilmore, *Lie Groups, Lie Algebra, and Some of Their Applications* (Dover, New York, 2005).
[28]Y. Yamasaki, S. Miyasaka, Y. Kaneko, J.-P. He, T. Arima, and Y. Tokura, Phys. Rev. Lett. **96**, 207204 (2006).
[29]M. Kenzelmann, A. B. Harris, S. Jonas, C. Broholm, J. Schefer, S. B. Kim, C. L. Zhang, S.-W. Cheong, O. P. Vajk, and J. W. Lynn, Phys. Rev. Lett. **95**, 087206 (2005).
[30]M. Uchida, Y. Onose, Y. Matsui, and Y. Tokura, Science **311**, 359 (2006).
[31]J. H. Han, J. Zang, Z. Yang, J.-H. Park, and N. Nagaosa, Phys. Rev. B **82**, 094429 (2010).